

1 Article

2 Characteriation of material properties based on 3 inverse finite element modelling

4 Mikdam Jamal ^{1*} and Michael N. Morgan ²

5 ¹ The Manufacturing Technology Centre Ltd., Ansty Park, Coventry CV7 9JU, UK; Mikdam.Jamal@the-
6 mtc.org

7 ² Advanced Manufacturing Technology Research Laboratory (AMTREL), Faculty of Engineering and
8 Technology (FET), Liverpool John Moores University, Liverpool L3 3AF, U

9 * Correspondence: Mikdam.Jamal@the-mtc.org

10

11 **Abstract:** This paper describes a new approach that can be used to determine the mechanical
12 properties of unknown materials and complex material systems. The approach uses inverse finite
13 element modelling (FEM) accompanied with a designed algorithm to obtain the modulus of elasticity,
14 yield stress and strain hardening material constants of an isotropic hardening material model, as well
15 as the material constants of the Drucker-Prager material model (modulus of elasticity, cap yield stress
16 and angle of friction).

17 The algorithm automatically feeds the input material properties data to finite element software and
18 automatically runs simulations to establish a convergence between the numerical loading-unloading
19 curve and the target data obtained from continuous indentation tests using common indenter
20 geometries. A further module was developed to optimise convergence using an inverse FEM
21 analysis interfaced with a non-linear MATLAB algorithm.

22 A sensitivity analysis determined that the dual Spherical and Berkovich (S&B) approach delivered
23 better results than other dual indentation methods such as Berkovich and Vickers (B&V) and Vickers
24 and Spherical (V&S). It was found that better convergence values can be achieved despite a large
25 variation in the starting parameter values and / or material constitutive model and such behaviour
26 reflects the uniqueness of the dual S&B indentation in predicting complex material systems.

27 The study has shown that a robust optimization method based on a non-linear least-squares curve
28 fitting function (LSQNONLIN) within MATLAB and ABAQUS can be used to accurately predict a
29 unique set of elastic plastic material properties and Drucker-Prager material properties. This is of
30 benefit to the scientific investigation of properties of new materials or obtaining the material
31 properties at different location of a part which might be not be similar due to manufacturing
32 processes (e.g. different heating and cooling rates at different locations).

33 **Keywords:** Material charecterisation, Inverse Finite Element Material modelling, Elastic Plastic
34 material model, Drucker-Prager material model

35

36 1. Introduction

37 In this paper, outcomes of a research study concerned with the application of indentation
38 processes with different indenter geometries is reported. The aim of the study was to establish a
39 predictive capability for the elastic plastic material properties of various material systems and to
40 develop an accurate method for specific applications. Many researchers have suggested that a non-
41 unique set of mechanical properties can be predicted for strain hardening elastic plastic material from

42 a single indentation test. However, most proposed methods in literature have been characterised by
43 parameters of load displacement curves using two or more indenters to determine a unique set of
44 material properties [1-3].

45 FEM based algorithms using single and multiple indenters have been proposed by other
46 researchers to determine the mechanical properties of different engineering material systems. This
47 approach has been used on some complex or non-standard materials or surfaces, such as in-vivo
48 tension, and brittle indentation [4-6]. Two different approaches were established to investigate and
49 predict the elastic plastic material properties and other complex material constitutive laws. The first
50 approach predicts material properties based on the single indentation test, examined separately, all
51 indenters sharing the same initial start value. The application of such an approach, investigated by
52 many researchers, has failed to achieve high accuracy, because the range of tested material properties
53 produced non-identical load displacement curves. In some cases the accuracy of this approach could
54 be improved depending on the previous knowledge about the material [7-9].

55 The second approach predicts the material properties based on the dual indentation test. In this
56 approach two types of indenters with different shapes and dimensions are employed resulting in
57 different plastic strain profiles i.e. different load displacement curves. Chollacoop, Dao et al. [10]
58 applied a modified single indenter algorithm to two and more indenter shapes. Dao, Chollacoop et
59 al. [8] developed forward analysis which considered that the representative stress and strain and the
60 loading curvature were functions of the face angle of the conical indenter. The inverse algorithm then
61 used the second pair of representative stress and strain values in order to obtain the unknown
62 mechanical properties. The algorithm showed significant improvements in the predicted Yield stress,
63 σ_y and strain hardening exponent 'n', compared to single indenter.

64 Yan, Karlsson et al. [11] used dual indenter geometries to determine the mechanical properties in
65 engineering materials. The modulus of elasticity and initial residual stress were assumed to be
66 known. They performed forward FEM simulations with dual indenters to predict the yield stress and
67 strain hardening. The result showed that the load displacement curves are more appropriate for the
68 prediction of yield strength than the single indenter geometry approach, with an error of less than
69 5%.

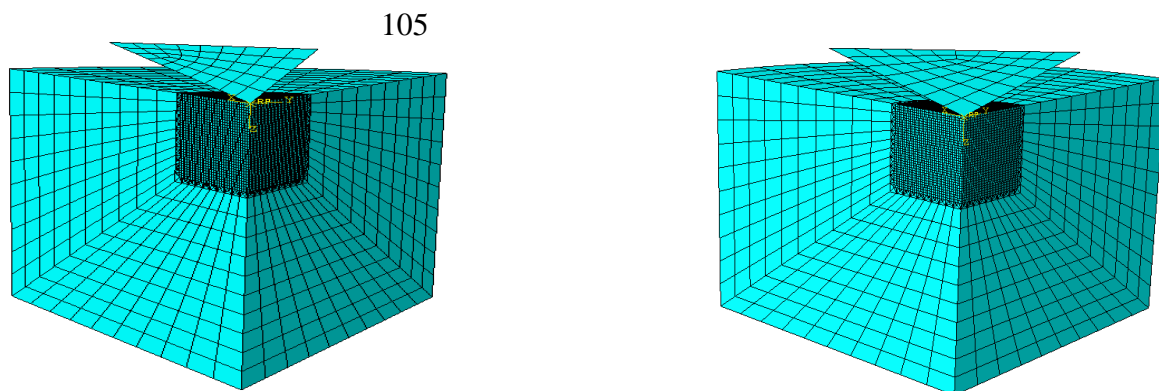
70 The research in this study is focused on alternative approaches that use inverse FEM
71 accompanied by an optimization algorithm to obtain and optimize the elastic plastic and Drucker-
72 Prager material properties. The proposed framework will enable the characterisation of complex
73 material systems. The main objective of this research is to develop a coupled computational method
74 based on FEM and an optimization algorithm to extract unique and accurate mechanical properties
75 for elastic plastic material model with isotropic hardening and Drucker-Prager material model from
76 full indentation loading unloading curves using dual indenter geometries. The second objective is to
77 examine the accuracy of the proposed inverse framework, coupled FEM with an optimization
78 algorithm technique, based on available load-displacement data.

79
80 The work consists of two main parts. In the first part, inverse FEM models of the continuous
81 indentation of commonly used 3-D indenter geometries (Vickers, Berkovich, and Spherical indenter)
82 were developed. In the second part, an inverse framework, FEM interfaced with a non-linear
83 MATLAB optimization algorithm, was developed based on the load displacement results of dual
84 indentation data. The effects of initially assigned values of the material properties and indenter

85 geometry were examined to investigate the robustness of the proposed optimisation framework. The
 86 optimization framework was then used to predict material properties by matching the load-
 87 displacement curves.

88 2 Finite element indentation models

89 Three-dimensional numerical models for three different axisymmetric rigid indenter geometries
 90 (Berkovich, Vickers, and Spherical) were developed in Abaqus to validate the optimization technique
 91 for various material systems. Figure 1 (a, and b) shows the 3-D Berkovich and Vickers indenter
 92 geometries, only 1/4 of symmetric specimens and indenters were performed, for both indenters. The
 93 planes of symmetric geometries are defined in the X-Z and Y-Z planes. All specimens and indenters
 94 were modelled with 8-node element type reduced integration (C3D8R), and 4-node element type
 95 rigid quadrilateral (R3D4) respectively. Both elements types are used for stress and displacement
 96 analysis. Figure 1 (c) shows 3-D spherical indenter where quarter of the specimen and indenter
 97 were modelled. Symmetry was defined on the X-Z and Y-Z planes. The specimen and indenter were
 98 modelled with 8-node reduced integration element (C3D8R) for the stress displacement analysis.
 99 The indentation method was simulated in two alternating steps (loading and unloading). During the
 100 loading step, the indenter was moved along in the z-direction in ramp mode and penetrated the
 101 specimen until the maximum depth is achieved. During the unloading step, the indenter was
 102 returned to the initial position. The reaction force was recorded at the indenter representing the total
 103 force during loading and unloading.
 104

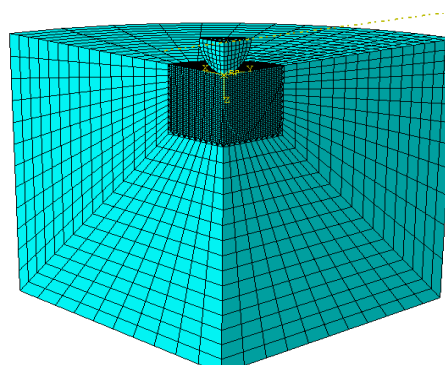


114
 115 (a)

116 **Figure 1(a)** FE model of Berkovich indentation

(b)

Figure 1 (b) FE model of Vickers indentation



127 (c)

128 **Figure 1 (c)** FE model of Spherical indentation

129 2.1. Elastic plastic material constitutive model

130 An elastic plastic material constitutive law was used in ABAQUS [12] to model the elastic and
131 plastic behaviour of metallic alloys [13]. The constitutive law used to simulate the indentation process
132 is shown in Eq.1. The elastic behaviour is modelled using Hooke's law while the plasticity is modelled
133 using isotropic strain hardening model described with a power function stress (σ), and strain (ϵ).

$$134 \quad \sigma = \begin{cases} E\epsilon, & \text{for } \sigma \leq \sigma_y \\ R\epsilon^n, & \text{for } \sigma \geq \sigma_y \end{cases} \quad (1)$$

135 For modelling of true stress and true strain behaviour, [13] proposed Eq. (2) to calculate the plasticity.

$$136 \quad \sigma_p = R \left(\frac{\sigma_y}{E} + \epsilon_p \right)^n \quad (2)$$

137 The material coefficient, R is given by:

$$138 \quad R = E^n \sigma_y^{1-n} \quad (3)$$

139 The four parameters (E, σ_y, ν, n) were used to optimize the elastic plastic material properties. The
140 Poisson's ratio and strain hardening exponent values span the range between 0 and 0.5 for most
141 engineering materials. However, in this study no lower and upper boundaries have been specified
142 for the values of Young modulus and Yield stress in order to represent a wide range of metallic and
143 ceramics material properties. A fixed set of plastic strain values of $0 < \epsilon_p \leq 0.3$ with 0.05 step
144 increment were used. The stress values were then updated for a given plastic strain value using Eq.
145 (2).

146 2.2. Drucker - Prager material constitutive model

147 Linear Drucker-Prager hardening constitutive material law was used to describe the indentation
148 response of material exhibiting hydrostatic stress sensitivity behaviour. Such a model can be used to
149 describe the deformation behaviour of soils and granular materials, metallic glass, and polymer
150 materials [14]. The linear plastic Drucker-Prager model is given by Eq. (4):

$$151 \quad \sigma_e + \mu \sigma_m - \sqrt{3} \sigma_s = 0 \quad (4)$$

152 Where: $\sigma_e = \sqrt{\frac{3}{2} S_{ij} S_{ij}}$ is the Von Mises equivalent stress, and $S_{ij} = \sigma_{ij} - \sigma_m \epsilon_{ij}$ is the stress
153 deviator, $\sigma_m = \sigma_{kk}/3 = -p$, σ_s is the shear stress, μ is the hydrostatic stress sensitivity parameter,
154 and β is the friction angle. In ABAQUS, the Drucker-Prager material model is defined using the
155 angle of friction β , dilatation angle ψ , flow stress ratio K, and hardening curves for different strain
156 rates.

157 The angle of friction β can be determined from the hydrostatic stress sensitivity parameter while
158 μ is dependent on the adhesive material and characterises the sensitivity of yielding to hydrostatic
159 stress. The value of μ is determined from tests under two different stress states given by Eq. (5), using
160 yield stress from shear and tensile tests. The dilatation angle ψ can be determined from the flow
161 parameter μ^* from Eq. (6). Non-associated flow is defined when μ^* is not equal to μ while

162 associated flow is defined when μ^* equal to μ . In this study, an associated flow was assumed by
 163 setting μ^* equal to μ in ABAQUS.

$$164 \quad \tan \beta = \mu = 3[(\sqrt{3} \sigma_s / \sigma_T) - 1] \quad (5)$$

$$165 \quad \mu^* = \tan \psi = 3(1 - 2 \nu^p) / 2(1 + \nu^p) \quad (6)$$

166 Where ν^p is a plastic component of Poisson's ratio.

167 The third parameter required in ABAQUS is the flow stress ratio K , which defines the differences
 168 in material behaviour under tension and compression. Park, Xia et al. [15] considered the parameter
 169 K to be in the range of $0.788 \leq k \leq 1$ in order to ensure the convexity of the yield stress. However, the
 170 flow stress ratio used in this study for the material model was set to 1 assuming identical behaviour
 171 under tension and compression.

172 Three material parameters (E , σ_{yc} , β) have been used to optimize the Linear Drucker-Prager material
 173 model. In this study, no lower and upper limits have been specified for the values of Young modulus
 174 and compressive Yield stress. The friction angle values were selected to be in the range of $0 \leq \beta \leq 30^\circ$,
 175 with 0.1° space interval in order to represent a wide range of material properties.

176 3 Development of the optimization method

177 Many optimization methods have been used by researchers to predict the best parameters using
 178 single- or multi-objective functions, for example [16, 17]. The main purpose of the optimization
 179 techniques is the involvement of iteratively changing the material parameters by re-running the FEM
 180 until it achieves a best fit between the load displacement curve obtained from real measurement
 181 results and the curve obtained from numerical analysis. In this approach, an optimisation algorithm
 182 is coupled with the FEM in order to find the optimal values (minimum objective function) for a set
 183 for a wide range of material properties to be determined.

184 In this study an optimization algorithm has been developed to determine the material properties
 185 for a given set of indentation data using an iterative procedure in MATLAB (The Math Works Inc.).
 186 The non-linear least-squares optimization function (LSQNONLIN) was developed in MATLAB
 187 based on the Levenberg–Marquardt algorithm (Matlab). A special code was written in MATLAB
 188 including the optimisation function and commands to read input files, write output files and execute
 189 the ABAQUS solver. The optimisation process started by selecting arbitrary initial values for each
 190 parameter and then running the ABAQUS input file using these values for the particular material
 191 model. A python script was then used to extract the history of force and displacement which is read
 192 in MATLAB to compute the objective function.

193

194 The optimization algorithm based on the dual indentation method was also assessed to predict
 195 the elastic plastic material properties. In this case the new optimization algorithm was developed to
 196 allow two set of input data with different indenter types or size to be used. The MATLAB code was
 197 then used to automatically run two ABAQUS input files in order to iteratively determine the residual
 198 error between target and optimized load displacement curves. The residual error criterion is based
 199 on the use of objective function until minimum convergence value within the range of $0.001 \leq$
 200 $\min F(x) \leq 0.02$ is achieved. The objective function for dual indenters is defined by Eq. (7):

$$\begin{aligned} 201 \quad \min F(x) = & \frac{1}{2} \sum_{i=1}^n \left\{ \left[(F_{num-l}^i - F_{exp-l}^i)^2 + (F_{num-ul}^i - F_{exp-ul}^i)^2 \right]_{indenter1} + \left[(F_{num-l}^i - F_{exp-l}^i)^2 + \right. \right. \\ 202 \quad & \left. \left. (F_{num-ul}^i - F_{exp-ul}^i)^2 \right]_{indenter2} \right\} \end{aligned} \quad (7)$$

203 where, $x = (E, \nu, \sigma_y, \text{ and } n)$ for Elastic-Plastic material law

204 $x = (E, \nu, \sigma_{yc}, \text{ and } \beta)$ for Linear Drucker-Prager material law

205 Where $\min F(x)$ is the minimum objective function, x is the optimization parameter set. F_{exp-l}^i
 206 is the measured Force applied during loading at a particular depth, F_{num-l}^i is the value of Force
 207 obtained by the FEM at the same depth as in the experiment during loading, F_{exp-ul}^i is the measured
 208 Force in unloading at a particular depth, F_{num-ul}^i is the value of Force obtained by the FEM at the
 209 same depth as in the experiment during unloading, and n is the number of sampling points in each
 210 test.

211 In this method the objective function value was first calculated at each indentation point
 212 (displacement step) using a non-linear least-squares objective function (LSQNONLIN) in MATLAB,
 213 and then the sum of the objective functions were integrated over the whole indentation curve. The
 214 total objective function value for a given set of material parameters (σ_y, E, ν, n) was calculated by the
 215 summation the objective function of dual indenters at each iteration in the optimization algorithm.
 216 Figure 2 shows the optimization workflow for material characterization. In this workflow, the
 217 processing of input files were created, post processing to output database files, and then extracting
 218 the data to the .rpt files in Abaqus. The whole process was implemented into the automated algorithm
 219 for the final stage of inverse FEM analysis by a non-linear least square data fitting optimization tool.

220

221

222

223

224

225

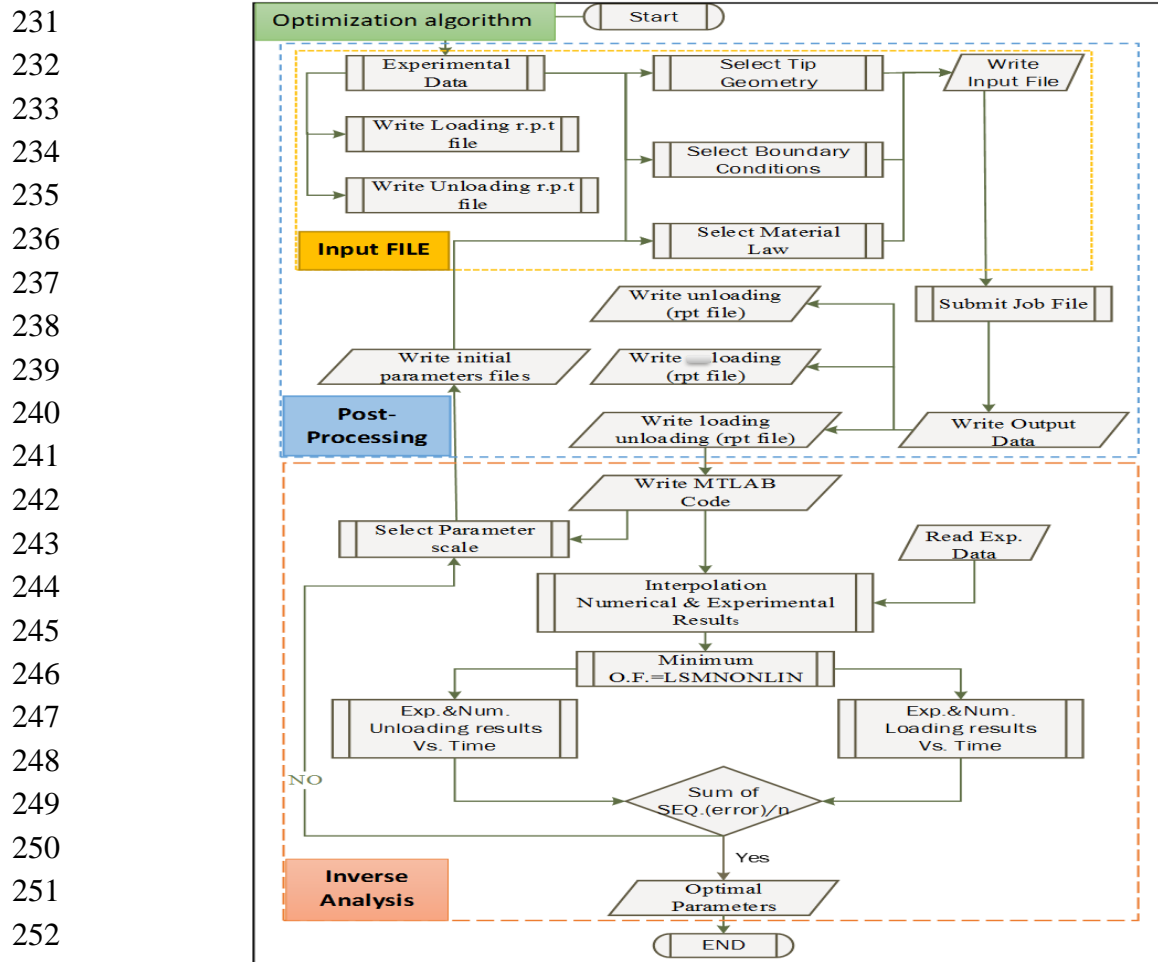
226

227

228

229

230



254 **Figure 2** Optimization workflow for material characterization

255 4. Results

256 4.1. Optimization analysis of elastic plastic material properties based on dual indenter geometries

257 The optimization algorithm was carried out using 3-D indenter geometries (Berkovich, Vickers
258 and Spherical) to predict the material properties of an elastic plastic target material. Figure 3 shows
259 the target numerical load displacement curve for pure Aluminum material with known mechanical
260 properties ($\sigma_y = 550\text{MPa}$, $E = 72\text{GPa}$, $\nu = 0.22$, $n = 0.1$) (Chollacoop, Dao et al. 2003), which is used
261 as blind test numerical data based on the indentation process of three different tip geometries.
262 Various ranges of initial guess were used to investigate the effect of starting point on the convergence
263 of results. The numerical load displacement data was divided into 50 equally spaced points against
264 the indentation force and used in the post-processing stage of the optimization workflow.

265 The numerical simulations of the target material show discrepancy in the loading unloading
266 curves for different indentation processes. These differences in the load displacement curves give a
267 good boundary to test the sensitivity and accuracy of the optimization algorithm of elastic plastic
268 materials. However, in order to validate the optimization algorithm in more depth, indentation
269 hardness HIT (Eq. 8), effective elastic modulus, E_{eff} (Eq. 9) and indentation depth ratio (final
270 indentation depth to the maximum indentation depth) which represents the depth ratio of target
271 material $(h_{max}/h_f)_T$ divided by the depth ratio of optimized material $(h_{max}/h_f)_O$ (Eq. 10), can be

272 calculated from the optimal loading unloading curve using the Oliver and Pharr method and
 273 compared with results obtained from target loading unloading curves.

274 Indentation hardness:

$$275 \quad H_{IT} = \frac{F}{A_P} \quad (8)$$

276 Effective elastic modulus:

$$277 \quad E_{eff} = \frac{\sqrt{\pi} S}{2\beta \sqrt{A_P}} \quad (9)$$

278

279 Depth ratio:

$$280 \quad 281 \quad (h_{max}/(h_f)_t)/(h_{max}/(h_f)_{opt}) \quad (10)$$

282 In this case, the sensitivity of this algorithm was examined by changing four material parameters
 283 (σ_y , E , ν , and n). Other parameters related to the specimen geometry and size, boundary conditions
 284 and applied load are fixed for all numerical simulations. The Young's modulus, Yield stress, Poisson's
 285 ratio, and strain hardening values were selected within the range of $10 \leq E \leq 150$ GPa, $100 \text{ MPa} \leq$
 286 $\sigma_y \leq 3$ GPa, $0.05 \leq \nu \leq 0.5$, and $0 \leq n \leq 0.5$, respectively. The optimization results are summarised in
 287 Table 1. The initial guess set was selected randomly from a range of material properties for various
 288 types of dual indenter numerical simulations. However, the percentage errors between the predicted
 289 results for a particular parameter and the target results for the same parameters can be calculated
 290 using the following expression Eq. (11):

$$291 \quad Residual \ error \ \% = \left[\left| 1 - \frac{predicted \ result - target \ result}{target \ result} \right| \right] \times 100 \ \% \quad (11)$$

292 The initially prescribed mechanical properties for an elastic plastic hardening material model
 293 (σ_y , E , ν , n) were randomly changed in order to examine the sensitivity of this method. Table 1
 294 summarises the optimization results of three different dual indenter geometries: Berkovich and
 295 Vickers (B&V), Vickers and Spherical (V&S), and Spherical and Berkovich (S&B). The initial guesses
 296 were selected from a wide range of material property sets for various dual numerical simulations.

297

298

299

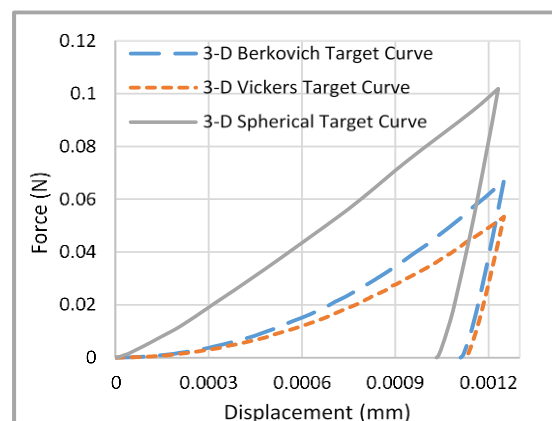
300

301

302

303

304



305 **Figure 1** Target numerical load displacement curves determined from 3-D simulations for Berkovich
 306 indentation, Vickers indentation, and Spherical indentation

307 The optimization analysis based on dual indenter geometries suggested that the four parameters
 308 (σ_y, E, ν, n) achieved convergence at different iteration numbers to within 2% of the target values
 309 regardless of the starting point. The result also shows that the objective function between the target
 310 and predicted load displacement curves was less than 1%. The optimized modulus of elasticity and
 311 strain hardening values are in excellent agreement with the target values. This suggests that the
 312 elastic plastic material properties can be accurately obtained by the proposed optimization technique
 313 of dual indenter geometries.

314 In order to examine the accuracy of the proposed method Table 1 presents the calculation of the
 315 normalized hardness ratio HT/HO (target indentation hardness / optimized indentation hardness),
 316 and normalized Reduced modulus ratio $(Er)T/(Er)O$ (target reduced modulus / optimized reduced
 317 modulus). The results show that the maximum percentage error was about 1% in the reduced
 318 modulus and the hardness ratio over indentation techniques.

319 Figure 4 shows the convergence trends of the five initial guess values of elastic plastic materials.
 320 The results clearly illustrate that the initial guess values of elastic plastic hardening material models
 321 can converge to their target values by the dual indentation optimization algorithm, but with different
 322 iteration numbers. It is worth noting that additional analyses were also investigated using a wide
 323 range of initial guess values. It was found that the application of the proposed algorithm was more
 324 reliable for any initial guess values within the defined database i.e. ($1 \leq E \leq 220$) GPa, $100 \text{MPa} \leq$
 325 $\sigma_y \leq 3 \text{GPa}$, $0 \leq n \leq 6$, $0.05 \leq \nu \leq 0.5$.

326

327 **Table 1** Dual indenter optimization results of elastic plastic material

Indenter	Parameter	Target value	Initial value	Predicted value	Error %	HT/H O	(Er)T/(Er)O	Depth ratio
(3-D)	E(GPa)	72	10	72.71	0.99	0.992	0.996	0.98
Berkovich	σ_y (MPa)	550	260	540	1.85			
&	ν	0.22	0.14	0.222	1.2			
Vickers	n	0.1	0.01	0.099	0.99			
(3-D)	E(GPa)	72	90	72.43	0.59	0.997	0.992	0.978
Vickers	σ_y (MPa)	550	260	543	1.28			
&	ν	0.22	0.35	0.222	1.25			
Spherical	n	0.1	0.05	0.099	0.87			
(3-D)	E(GPa)	72	50	72.22	0.30	0.990	0.994	0.986
Spherical	σ_y (MPa)	550	440	546	0.47			
&	ν	0.22	0.2	0.222	1.11			
Berkovich	n	0.1	0.01	0.101	1.01			

328

329

330

331

332

333

334

335

336

337

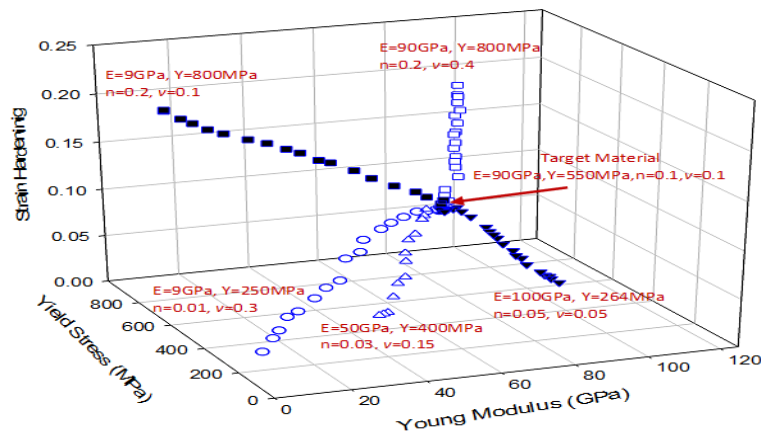
338

339

340

341

342



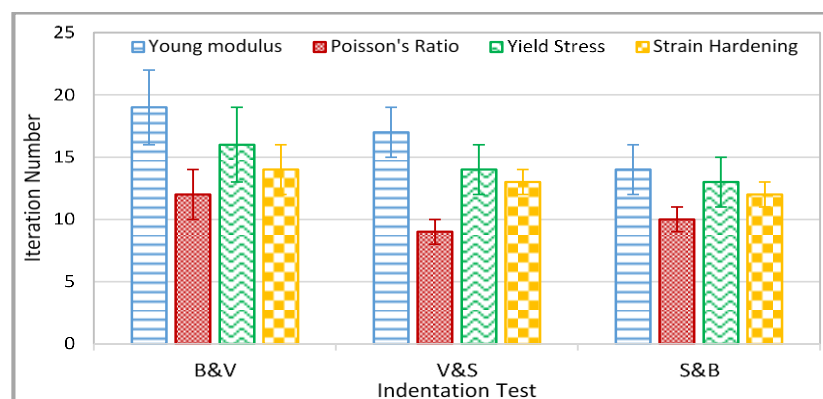
(a) Elastic plastic hardening target material

343 **Figure 4** Converging trends of five initial guess values using S&B dual indenter for a) elastic plastic hardening
344 target material.

345 Figure 5 shows the optimization history of the material properties from initial guess values to
346 their target values (with 0.01 residual error) based on three different dual indentation tests (B&V),
347 (V&S), and (S&B). The average convergence history of the indentation tests shows that the four
348 parameters achieved the target values after 19, 17, and 14 iterations respectively over a range of initial
349 guess material properties. The error bar presented in each column explains that material properties
350 can reach their target values at different number of iterations, these variations depending on initial
351 guess values.

352 The optimization process, based on the S&B indentation test, provides the best solution because
353 fewer iterations are required for the main parameters (σ_y , E , and n) to achieve convergence. It can be
354 clearly noticed that the Poisson's ratio required less iterations to achieve convergence; however the
355 results are not affected due to the fewer influence of this parameter on the load displacement curve,
356 whereas the Young's Modulus required a high number of iterations to achieve convergence followed
357 by the Yield stress and then the strain hardening.

358



359

360 **Figure 5** Optimization results of elastic plastic material properties based on s (B&V), (V&S), (S&B) indentation
361 test.

362

363 4.1.1. Sensitivity analysis of elastic plastic optimization algorithms

364 The sensitivity of the optimization process used to predict elastic plastic material properties as
365 a result of continuously changing the input parameters until achieving a best match between
366 predicted and experimental is a major difficulty in using the inverse or reverse method [18]. In this
367 study, series of input target materials were employed to investigate the sensitivity and accuracy of
368 the optimization algorithm based on S&B, B&V, and V&S indentation methods. However, in the
369 actual experimental work, there are many factors which potentially cause systematic and random
370 error. These errors may be related to indenter deformation and tip blunting during indentation, as
371 well as the accuracy of the indentation measurements [8].

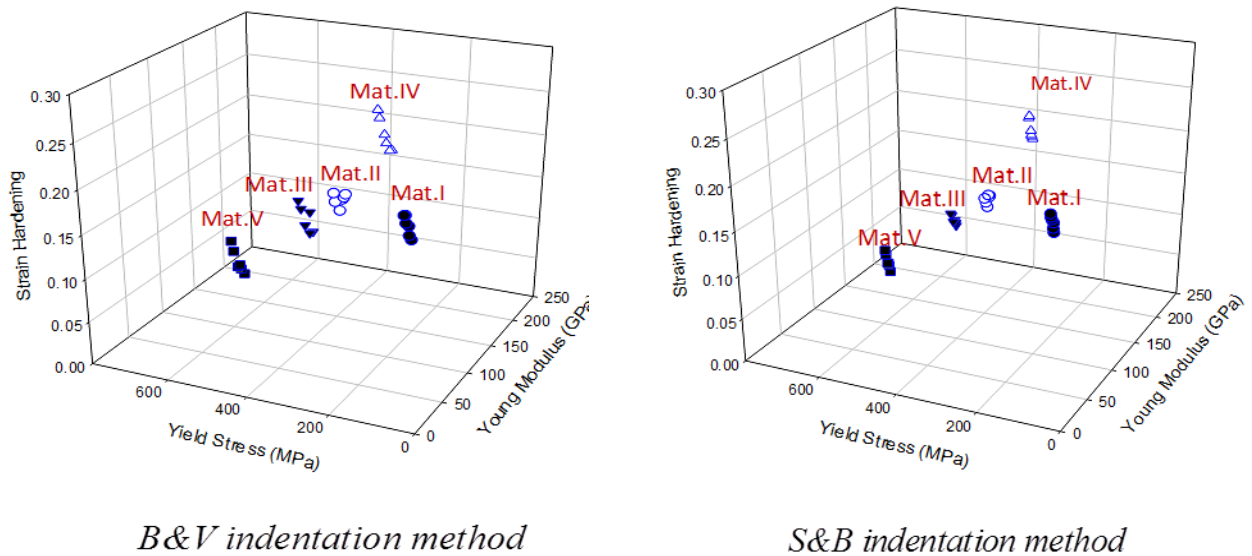
372 Figure 6 shows the sensitivity analysis of three optimization methods with five different sets of
373 material properties which have been used as input data to evaluate the accuracy and sensitivity of
374 the approaches. In each approach, there are only a few material property sets that match the target
375 data and all parameters are focused in a small boundary region. As displayed, the results achieved
376 by the S&B approach is significantly better than the other methods (B&V, and V&S) because the
377 boundary regions are smaller. A small deviation in the predicted mechanical properties
378 (σ_y , E , and n) produces a very limited material range with identical load displacement curves (same
379 objective function); such behaviour reflects the uniqueness of the method in solving complex material
380 systems.

381 Table 2 summarizes the sensitivity analysis of the S&B optimization method applied on five
382 different sets of material properties using theoretical values. The results from each set of parameters
383 represent the residual error between the target and predicted load displacement curves to within \leq
384 2% determined by the non-linear least-squares objective function (LSQNONLIN) in MATLAB. The
385 previous analysis shows that the Poisson's ratio has less influence on the predicted load displacement
386 curves, therefore only three parameters (σ_y , E , and n) were used in the optimization algorithm.
387 In the case of the S&B approach, the deviation and percentage error of E calculated during the
388 sensitivity analyses for a range of materials were within 2.6 GPa, and 1.6% respectively. The deviation
389 and percentage error of σ_y were within 6.5 MPa, and 1.1% respectively, while the percentage error
390 of n was within 0.001, and 1.2% respectively. This suggests that the Elastic modulus, Yield stress, and
391 strain hardening can be extracted using the proposed method within 1.6%, 1.1%, and 1.2% relative
392 error respectively. All the proposed parameters can be determined with a specific percentage of
393 errors if the load displacement curves are measured with accuracies greater than 98%. This indicates
394 that the accuracy of the measured load displacement curve is important to predict an accurate
395 material properties. However, the results achieved is significantly better than some stated methods
396 in the previous works [8].

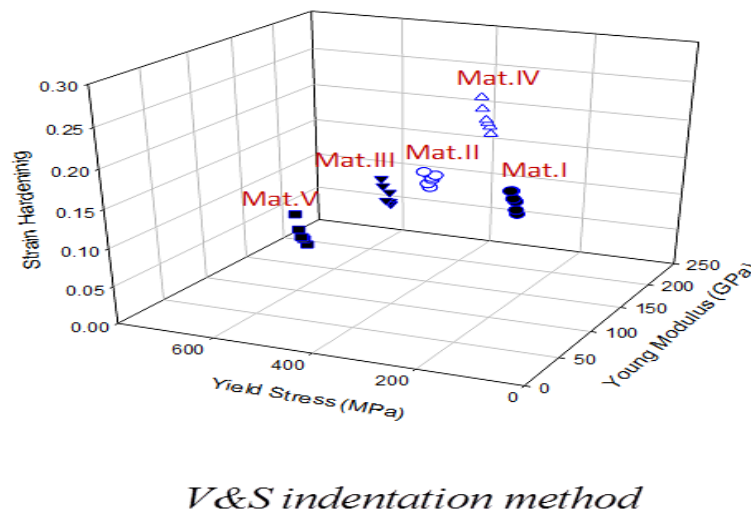
397 The true stress-strain curves with optimal predicted material properties (minimum objective
398 function) were plotted in Figure 7, which shows that these stress-strain curves are identical. Figure 8
399 compares the load displacement curves of optimal material property sets with the input target data
400 ($\sigma_y = 550 \text{ MPa}$, $E = 80 \text{ GPa}$, $\nu = 0.2$, $n = 0.09$).

401
402
403

404 The load displacement curves of the predicted material properties agree very well with the target
 405 material, all parameters being focused in a small boundary region to within $\leq 2\%$ residual errors.
 406 This suggests the optimization algorithm based on the pair of Spherical and Berkovich` indentations
 407 can accurately predict the elastic plastic material properties with unique stress-strain curves.
 408



409



410
 411
 412
 413
 414
 415
 416
 417
 418
 419
 420
 421
 422
 423
 424
 425
 426
 427

Figure 6 Sensitivity and accuracy results of elastic plastic optimization algorithms (S&B, B&V, and V&S)

428 **Table 2** Sensitivity and accuracy analysis of S&B optimization method

Material	Parameter	Theoretica l value	Initial value	Predicted value	Error %
Mat.I	E(GPa)	100	40	100.9	0.82
	σ_y (MPa)	160	100	161.2	0.71
	ν	0.2	0.2	0.2	0
Mat.II	E(GPa)	120	60	121.4	1.1
	σ_y (MPa)	350	175	346.6	0.98
	ν	0.2	0.2	0.2	0
Mat.III	E(GPa)	160	70	157.4	1.6
	σ_y (MPa)	500	250	544.5	1.1
	ν	0.2	0.2	0.2	0
Mat.IV	E(GPa)	200	110	202.4	1.2
	σ_y (MPa)	350	150	353.4	0.98
	ν	0.2	0.2	0.2	0
Mat.V	E(GPa)	80	10	79.2	1.0
	σ_y (MPa)	550	100	556.5	1.1
	ν	0.2	0.2	0.2	0

429

430

431

432

433

434

435

436

437

438

439

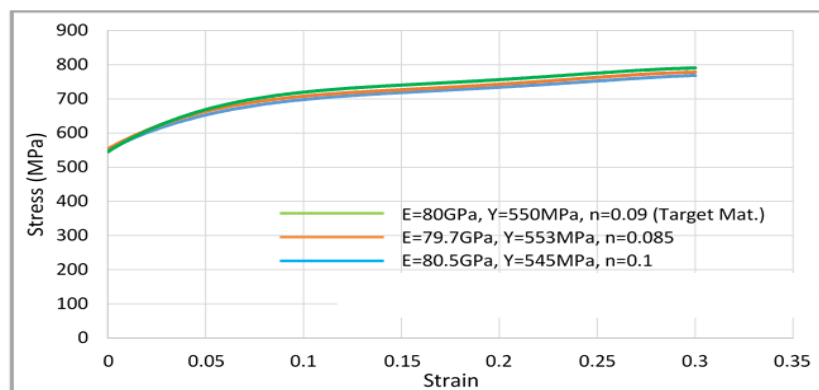
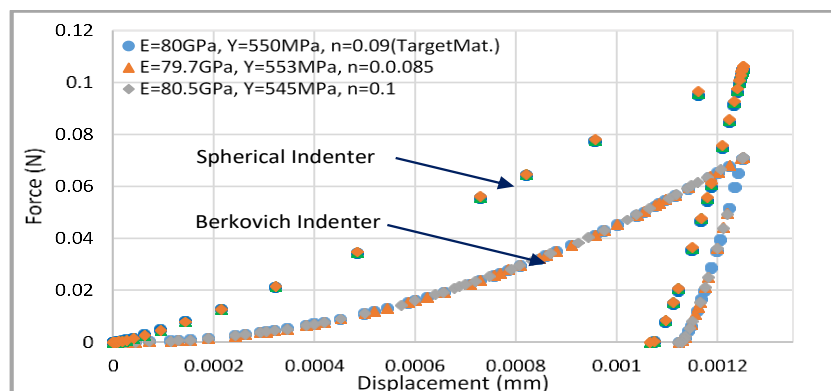


Figure 7 True stress-strain curves of target material and other data with objective function ≤ 0.01

440

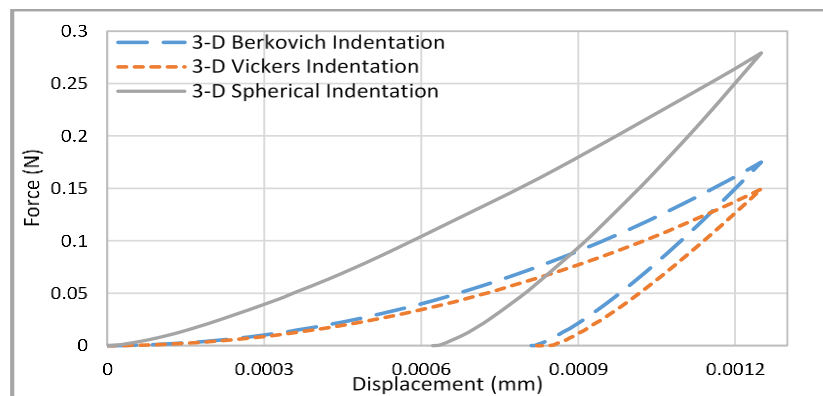


441 **Figure 8** Comparison between the predicted load displacement curves using the optimal and target material

442 properties for S&B approach

443 4.2 Optimization analysis of drucker-prager material properties based on dual indenter geometries

444 The optimization algorithms based on the dual indentation method were developed to predict
 445 the Linear Drucker-Prager material properties as well. The optimization algorithms were carried out
 446 using the same procedure and principles used in the dual indenter geometries for elastic plastic
 447 materials. Combinations of 3-D indenter geometries (Berkovich, Vickers and Spherical) were
 448 performed to predict the Drucker- Prager material behaviour. Various ranges of initial guess have
 449 been used to investigate the accuracy and sensitivity analysis of the proposed approaches. Figure 9
 450 shows the target load displacement curves for Bulk Metallic Glasses (BMG) obtained numerically
 451 with known mechanical properties ($\sigma_{yc} = 1640 \text{ MPa}$, $E = 72 \text{ GP}$, $\nu = 0.22$, $\beta = 30$, $\psi = 30$, and $k =$
 452 1) [19].



453

454 **Figure 9** Target Drucker-Prager numerical load displacement curves determined from 3-D FEM simulations
 455 for a) Berkovich b) Vickers and c) Spherical indentations

456 **Table 3** Dual indenter optimization results of hydrostatic stress sensitive (BMG) material

Indenter	parameter	Target value	Initial value	Predicted value	Error %	HT/H O	(Er)T/(Er)O	Depth ratio
3-D (B&V)	E(GPa)	72	50	73.39	1.89	0.97	0.96	0.97
	σ_{yc} (GPa)	1.64	1	1.61	1.82			
	β	300	150	30.4	1.31			
3-D (V&S)	E(GPa)	72	90	73.26	1.72	0.98	0.97	0.98
	σ_{yc} (GPa)	1.64	1	1.62	1.23			
	β	300	400	29.8	0.6			
3-D (S&B)	E(GPa)	72	10	72.94	1.28	0.985	0.99	0.984
	σ_{yc} (GPa)	1.64	1	1.62	1.23			
	β	300	0.050	30.2	0.7			

457

458

459 The optimization processes include three different pairs of indenter geometries (B&V), (V&S),
 460 and (S&B). The initial guess mechanical properties of Linear Drucker-Prager hardening material (E ,
 461 σ_{yc}, β) were changed a number of times in each process in order to investigate the sensitivity of this
 462 method. Table 3 summarises the optimization results of three different indentation tests based on the
 463 dual indentation methods on the BMG material.

464 The initial guess material properties were selected from a range of material property sets for
 465 various dual numerical simulations. The optimization algorithms were carried out by automatically
 466 changing the material properties in the ABAQUS input file (.inp) of each iteration until the objective
 467 function between the target and predicted load displacement curves achieved the minimum
 468 convergence value within the range of $0.001 \leq \min F(x) \leq 0.02$. Despite using a range of initial guess
 469 parameters, the variables (E, σ_{yc}, β) can converge to their target values at different iteration
 470 numbers to within a 2% percentage error. The optimized reduced modulus and hardness ratio are in
 471 good agreement with the target values. This suggests that the linear Drucker-Prager material
 472 properties can be accurately obtained by the proposed optimization techniques of dual indenter
 473 geometries.

474 Figure 10 shows the convergence trends of five initial guess values of hydrostatic stress sensitive
 475 plastic to their target material using the S&B indentation technique. The results demonstrated that
 476 the initial guess values could converge to their target values by the dual indentation optimization
 477 algorithm with different number of iterations. The materials with less difference between the initial
 478 and target values (i.e. availability of prior knowledge) will require fewer iterations to achieve
 479 convergence. Additional analyses were also investigated using a wide range of initial guess values.
 480 It was found that the application of the proposed algorithm is more reliable for any initial guess
 481 values within the defined database i.e. $1\text{GPa} \leq E \leq 150\text{GPa}$, $100\text{MPa} \leq \sigma_y \leq 5\text{GPa}$, $0^\circ \leq \beta \leq 30^\circ$, and
 482 $0.05 \leq \nu \leq 0.5$.

483 It should be noted that the most important challenge of such an optimization algorithm is to
 484 identify the accuracy of the final predicted material property values based on real experimental tests
 485 for new materials where target values may be unknown. However, the solution of repeating the
 486 process several times with different initial guess values can overcome this problem and ensure the
 487 repeatability of numerical simulations.

488

489

490

491

492

493

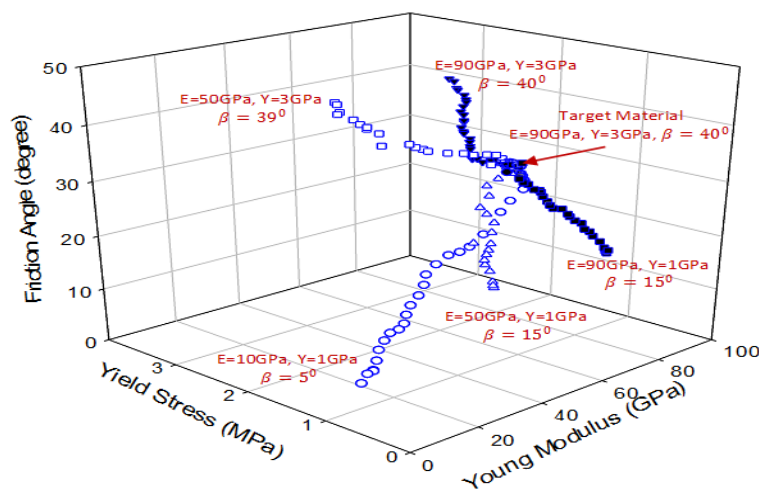
494

495

496

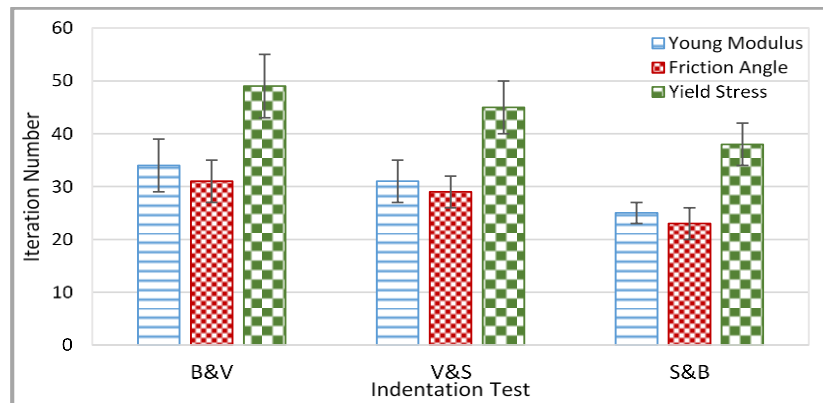
497

498



497 **Figure 10** Converging trends of five initial guess values using S&B dual indenter for pressure-sensitive plastic
 498 material properties

499 Figure 11 shows a comparison between three dual indentation methods concerning the
 500 optimization history of the initial guess material properties to their target values. The average
 501 convergence history of the B&V, V&S, and S&B indentation tests shows that the three parameters
 502 achieved their target values after 49, 45, and 38 iterations respectively, over a range of initial guess
 503 material properties. The error bar presented in each column explains that the material properties can
 504 reach their target values at different iteration numbers depending on initial guess values. The
 505 optimization process based on the S&B indentation test provide the best solution, because fewer
 506 iterations are required for the main parameters (E, σ_{yc}, β) to achieve convergence.



507

508 **Figure 11** Optimization history of (E, σ_{yc}, β) based on (B&V), (V&S), and (S&B) indentation test

509

510 4.2.1 Sensitivity analysis of drucker-prager optimization algorithms

511 A series of FEM simulations were developed to examine the accuracy and sensitivity of the
 512 optimization algorithms based on S&B, B&V, and V&S indentation methods using a range of
 513 hydrostatic stress sensitive plastic material properties. Table 4 presents the material properties of
 514 bulk metallic glass BMG material used in the numerical simulations. The material sets were employed
 515 as an input target data (blind test data) to evaluate the accuracy and sensitivity of the methods.

516 Figure 12 shows the sensitivity analysis of three optimization methods with four different sets of
 517 BMG material properties presented in Table 4. As presented, there are few material property sets that
 518 match the target data with the minimum objective function, and all parameters are concentrated in a
 519 small boundary region. The residual errors between target values and optimized parameters are
 520 various according to the optimization algorithm type, however the results achieved by the S&B
 521 method are significantly better compared with the other methods. The maximum relative errors were
 522 estimated as 7.5%, 6%, and 3.5% in the B&V, V&S, and S&B respectively. Consequently, the predicted
 523 properties (E, σ_{yc}, β) produce a very limited material range having identical load displacement
 524 curves (same objective function); such behaviour reflects the uniqueness of the method in solving
 525 complex material systems. However, the satisfactory existence of uniqueness and stability can
 526 suggest of considering the proposed method as a well-posed optimization solution.

527

528

529

530

531 **Table 4** Bulk metallic glass material properties

Material	E (GPa)	σ_{yc} (GPa)	β (degree)	ν	k	ψ (degree)	References
BMG I	124	2.01	40	0.25	1	40	(Inoue, Zhang et al. 2001)
BMG II	92	1.34	36	0.23	1	36	(Saida, Kato et al. 2007)
BMG III	74	1.78	35	0.23	1	35	(Yuan, Zhang et al. 2003)
BMG IV	52	1.08	32	0.22	1	30	(Inoue, Zhang et al. 1989)

532

533

534

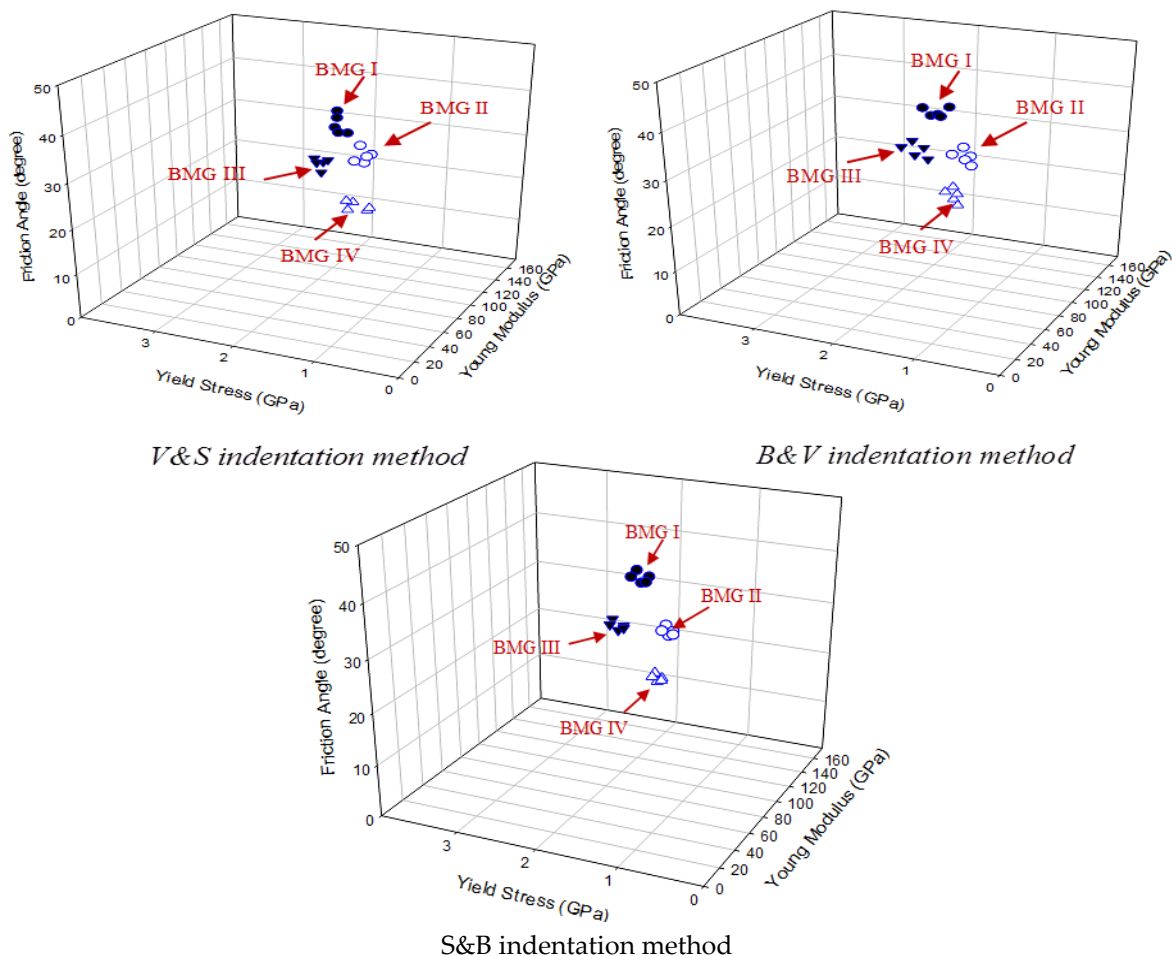
535

536

537

538

In the case of the S&B optimization algorithm, the convergence of Elastic modulus E, Yield stress σ_{yc} and Friction angle β for the examined materials was within 4%, 3.65%, and 4.2%, respectively. This demonstrated that the material properties E, σ_{yc} , and β can be extracted using the proposed method to within 4%, 3.65%, and 4.2% relative error, respectively. All the proposed parameters can be determined with a specific percentage of errors if the load displacement curves are measured with accuracies greater than 97%.



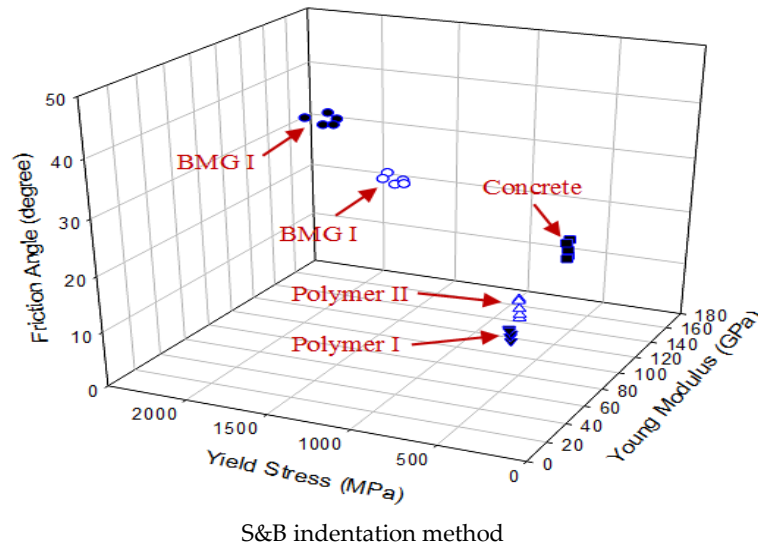
539

540

541

Figure 13 illustrates that there are a few material data sets over a small region matching the input data. This suggests that the combination of Spherical and Berkovich indenters could produce unique results.

542 The sensitivity analysis of the dual indentation S&B optimization algorithm was expanded to
 543 include other material systems such as ceramics, polymers, concrete and BMG. Table 5 summarizes
 544 the several material properties (E , σ_{yc} , β) used as input data to numerical simulations. The relative
 545 error for each parameter was measured at the best match between the predicted and target load
 546 displacement curves to within an accuracy of less than 3% determined by the non-linear least-squares
 547 objective function LSQNONLIN.

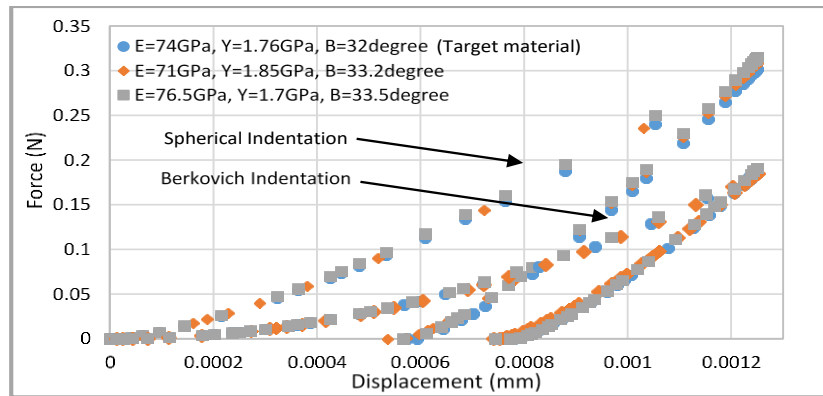


558 **Figure 13** Sensitivity and accuracy results of S&B optimization algorithms

559 **Table 5** Sensitivity and accuracy analysis of S&B optimization method

Material	Parameter	Target value	Initial value	Predicted value	Error %
Polymer I (Seltzer, Cisilino et al. 2011)	E(GPa)	5	0.5	5.18	3.4
	σ_{yc} (MPa)	140	10	144.5	3.2
	β	0	20	22	9
Polymer II (Seltzer, Cisilino et al. 2011)	E(GPa)	3.5	0.25	3.65	4.2
	σ_{yc} (MPa)	90	10	92.61	2.9
	β	0	25	23	8.6
Concrete (Mokhatar and Abdullah 2012)	E(GPa)	40	3	38.2	4.5
	σ_{yc} (MPa)	40	5	41.56	3.9
	β	0	30	31.5	5
BMG I (Inoue, Zhang et al. 2001)	E(GPa)	124	10	127.72	3
	σ_{yc} (MPa)	2010	300	2076	3.3
	β	0	35	32.9	4.7
BMG II (Saida, Kato et al. 2007)	E(GPa)	92	5	89.5	2.7
	σ_{yc} (MPa)	1340	200	1380	3
	β	0	30	28.65	4.5

560 Figure 14 Shows comparison of load displacement curves between the predicted and input
 561 target data ($\sigma_y = 1.76 \text{ GPa}$, $E = 74 \text{ GPa}$, $\nu = 0.22$, $\beta = 32^\circ$). It is clearly demonstrated that the load
 562 displacement curves using the predicted material properties agree very well with the input numerical
 563 target data. This suggests that the optimization algorithm based on dual of Spherical and Berkovich
 564 indentations can be accurately predict the hydrostatic stress sensitive plastic material properties.
 565



566
 567
 568
 569
 570
 571
 572
 573 **Figure 14** Comparison of load displacement curves between the predicted and target pressure-sensitive plastic
 574 material properties using S&B approach

575

576 5. Conclusion

577 In this study, an optimization algorithm was developed to extract the mechanical properties of
 578 for a given set of indentation data using a non-linear least-squares curve fitting function
 579 (LSQNONLIN) within the optimization toolbox of MATLAB based on the Levenberg–Marquardt
 580 algorithm. A special code was written in MATLAB including optimization algorithm and functions
 581 to read ABAQUS input files, write results files and execute ABAQUS. The optimization process
 582 started by selecting arbitrary initial values for the material paterial and then running ABAQUS
 583 models. A python script was then used to extract the history of load displacement data which was
 584 used to compute the objective function. The process runs iteratively until the best fit is achieved
 585 between predicted and experimental load displacement curves, This is achieved when the objective
 586 function reaches its minimum set by the convergence criteria. The optimum values of the parametrs
 587 are selected when best fit between numerical and experimental or target data is achieved.

588 The dual indentation optimization process was established to predict the mechanical properties over
 589 a wide range of material constitutive laws (elastic plastic material model and Drucker-Prager material
 590 model) to investigate the effectiveness of the optimization techniques for a wide range of materials.
 591 The results also show that the Elastic modulus and Yield stress require more iterations to reach
 592 convergence compared with other parameters. The optimization history of the full set of material
 593 properties for different indentation technique clearly demonstrates that the dual indentation method
 594 delivers better convergence values despite a large variation in the starting parameter values and / or
 595 material constitutive model.

596 In this case, the S&B dual indentation approach and different initial guess material properties
 597 values were also used to investigate the robustness of the proposed optimization algorithm. The
 598 results shows that an accurate Young modulus, Yield stress and strain hardening were obtained and

599 compared with the traditional technique of the Oliver and Pharr method based on experimental load
600 displacement curve analysis. This is of benefit to the scientific investigation of properties of new
601 materials.

602 Acknowledgements

603 The authors wish to acknowledge the support and contributions of the Engineering and Sciences
604 Research Council (EPSRC), Innovate UK and industry partners.

605

606 References

- 607 1. Chollacoop, N., M. Dao and S. Suresh (2003). "Depth-sensing instrumented indentation with dual sharp
608 indenters." *Acta materialia* 51(13): 3713-3729.
- 609 2. Swaddiwudhipong, S., K. Tho, Z. Liu and K. Zeng (2005). "Material characterization based on dual
610 indenters." *International journal of solids and structures* 42(1): 69-83.
- 611 3. Luo, J., J. Lin and T. Dean (2006). "A study on the determination of mechanical properties of a power law
612 material by its indentation force–depth curve." *Philosophical magazine* 86(19): 2881-2905.
- 613 4. Meuwissen, M., C. Oomens, F. Baaijens, R. Petterson and J. Janssen (1998). "Determination of the elasto-
614 plastic properties of aluminium using a mixed numerical–experimental method." *Journal of Materials*
615 *Processing Technology* 75(1): 204-211.
- 616 5. Shan, Z. and A. M. Gokhale (2003). "Utility of micro-indentation technique for characterization of the
617 constitutive behavior of skin and interior microstructures of die-cast magnesium alloys." *Materials Science*
618 *and Engineering: A* 361(1): 267-274.
- 619 6. Ren X. J., S. C. W., Evans K. E., Dooling P. J., Burgess A. and Wiechers J. W. (2005). "Experimental
620 testing and numerical modelling of mechanical properties of the human skin." *International Foundation of*
621 *Society of Cosmetic Chemists (IFSCC)*, 1 95-98.
- 622 7. Giannakopoulos, A. E. and S. Suresh (1999). "Determination of elastoplastic properties by instrumented
623 sharp indentation." *Scripta Materialia* 40(10): 1191-1198.
- 624 8. Dao, M., N. Chollacoop, K. Van Vliet, T. Venkatesh and S. Suresh (2001). "Computational modeling of the
625 forward and reverse problems in instrumented sharp indentation." *Acta materialia* 49(19): 3899-3918.
- 626 9. Bucaille, J.-L., S. Stauss, E. Felder and J. Michler (2003). "Determination of plastic properties of metals by
627 instrumented indentation using different sharp indenters." *Acta materialia* 51(6): 1663-1678.
- 628 10. Chollacoop, N., M. Dao and S. Suresh (2003). "Depth-sensing instrumented indentation with dual sharp
629 indenters." *Acta materialia* 51(13): 3713-3729.
- 630 11. Yan, J., A. M. Karlsson and X. Chen (2007). "Determining plastic properties of a material with residual stress
631 by using conical indentation." *International journal of solids and structures* 44(11): 3720-3737.
- 632 12. ABAQUS, T. m. v., Pawtucket: Hibbit, Karlsson and Sorensen, Inc.
- 633 13. Swaddiwudhipong, S., J. Hua, K. Tho and Z. Liu (2006). "Equivalency of Berkovich and conical load-
634 indentation curves." *Modelling and Simulation in Materials Science and Engineering* 14(1): 71.
- 635 14. Keryvin, V. (2007). "Indentation of bulk metallic glasses: Relationships between shear bands observed
636 around the prints and hardness." *Acta materialia* 55(8): 2565-2578.
- 637 15. Park, S., Q. Xia and M. Zhou (2001). "Dynamic behavior of concrete at high strain rates and pressures: II.
638 Numerical simulation." *International journal of impact engineering* 25(9): 887-910.

- 639 16. Gérard, J.-M., J. Ohayon, V. Luboz, P. Perrier and Y. Payan (2005). "Non-linear elastic properties of the
640 lingual and facial tissues assessed by indentation technique: Application to the biomechanics of speech
641 production." *Medical engineering & physics* 27(10): 884-892.
- 642 17. Kang, J., A. Becker and W. Sun (2012). "Determining elastic-plastic properties from indentation data
643 obtained from finite element simulations and experimental results." *International Journal of Mechanical
644 Sciences* 62(1): 34-46.
- 645 18. T.A. Venkatesh, K. J. V. V., A.E. Giannakopoulos and S. Suresh (2000). "Determination of elasto-plastic
646 properties by instrumented sharp indentation: Guidelines for property extraction." *Scripta mater.* 42: 833-
647 839.
- 648 19. Seltzer, R., A. P. Cisilino, P. M. Frontini and Y.-W. Mai (2011). "Determination of the Drucker-Prager
649 parameters of polymers exhibiting pressure-sensitive plastic behaviour by depth-sensing indentation."
650 *International Journal of Mechanical Sciences* 53(6): 471-478.